

# Tropospheric Age-of-Air: Influence of SF<sub>6</sub> Emissions on Recent Surface Trends and Model Biases

Clara Orbe<sup>1</sup>, Darryn W. Waugh<sup>2</sup>, Stephen Montzka<sup>3</sup>, Edward J. Dlugokencky<sup>3</sup>, Susan Strahan<sup>4,5</sup>, Stephen Steenrod<sup>4,5</sup>, Sarah Strode<sup>4,5</sup>, James W. Elkins<sup>3,7</sup>, Bradley Hall<sup>3</sup>, Colm Sweeney<sup>3</sup>, Eric J. Hinsta<sup>3,6</sup>, Fred L. Moore<sup>3,6</sup>, Emma Penafiel<sup>2</sup>

<sup>1</sup> NASA Goddard Institute for Space Studies; <sup>2</sup> Department of Earth and Planetary Sciences, Johns Hopkins University; <sup>3</sup> Global Monitoring Laboratory, NOAA; <sup>4</sup> Universities Space Research Association; <sup>5</sup> Atmospheric Chemistry and Dynamics Laboratory, NASA Goddard Space Flight Center; <sup>6</sup> Cooperative Institute for Research in Environmental Sciences (CIRES), University of Colorado Boulder; <sup>7</sup> Currently Retired

## Introduction

The mean time since air last contacted the midlatitude surface layer of the Northern Hemisphere (NH) (the mean age from the NH surface (Waugh et al. (2013)) is a fundamental measure of tropospheric transport. The mean age is not directly observable but can be estimated from measurements of SF<sub>6</sub> to derive an "SF<sub>6</sub> age" ( $\Gamma_{SF_6}$ ), or the time lag since the SF<sub>6</sub> mixing ratio at a given location equaled the mixing ratio over a northern midlatitude source region. Single-model (Waugh et al. (2013), Wu et al. (2018)) and multi-model (Orbe et al. (2018), Yang et al. (2019)) studies indicate that the ages simulated in models are biased old, compared to observations. However, the origins of this age bias in models remains poorly understood.

Current observational estimates of the SF<sub>6</sub> age have been limited to one ocean basin, rendering it hard to identify the origin of SF<sub>6</sub> age biases in models. In addition, these estimates only span 1997-2011, too short to justify an analysis of age trends, although other studies have shown that observed interhemispheric exchange times decreased by ~0.2 years during 1996-1999 and ~0.15 years during 2004-2007 (Patra et al. (2011)).

Here we use an expanded network of surface SF<sub>6</sub> measurements from the NOAA Carbon Cycle Greenhouse Gases (CCGG) group that is much broader in its zonal coverage compared to previous studies and extends over the time period 1997-2018. We combine the new observational data with new targeted simulations that address the following questions:

- #1. How has  $\Gamma_{SF_6}$  changed over recent decades and what are the underlying drivers of these trends (emissions vs. transport)?
- #2. What is the driver of SF<sub>6</sub> age biases in models?

## Methods

### (1) SF<sub>6</sub> Age ( $\Gamma_{SF_6}$ )

We define the "SF<sub>6</sub> age" ( $\Gamma_{SF_6}$ ) at a particular location as the time since the SF<sub>6</sub> mixing ratio in the "source region" ( $\Omega$ ; here, the NH midlatitude surface between 30°N-60°N) equaled the mixing ratio at that location, i.e.,  $\chi(r, t) = \chi_0(t - \Gamma_{SF_6}(r, t))$  where  $\chi(r, t)$  is the SF<sub>6</sub> mixing ratio at location  $r$  and  $\chi_0$  is the mixing ratio in  $\Omega$ .

We define two reference series ( $\chi_0$ ) based on the mean (median) of SF<sub>6</sub> mole fractions at all (31) available surface sites spanning 30°N-60°N, denoted as  $[\chi]_{0,30N-60N}$  ( $< \chi >_{0,30N-60N}$ ).

### (2) SF<sub>6</sub> Observations

**Surface:** We use the monthly mean flask-air measurements from the NOAA/CCGG division going back to 1997. The (82) NOAA/CCGG sites considered here span the extratropics and multiple ocean basins, in contrast to the 12 stations examined in Waugh et al. (2013). The quoted uncertainty is ~0.04 ppt, which translates to age uncertainties of ~0.13 years.

**Vertical Profiles:** SF<sub>6</sub> measurements from all four Atmospheric Tomography Mission (ATom) campaigns are used. We use the merged 10-second SF<sub>6</sub> in-situ chromatographic measurements from the PAN and Other Trace Hydrohalocarbon Experiment (PANTHER) and the Unmanned Aircraft Systems Chromatograph for Atmospheric Trace Species (UCATS); the merged Programmable Flask Package (PFP) Whole Air Sampler measurements are also used, albeit integrated over longer time intervals. The SF<sub>6</sub> (SF<sub>6</sub> age) quoted uncertainty is ~0.05 ppt (~0.16 yr) and 0.08 ppt (0.26 yr) for PFP and UCATS/PANTHER.

### (3) Model Simulations:

We use two simulations (CTM-Fix, CTM) produced using the NASA Global Modeling Initiative (GMI) chemical transport model, which span 1980-2016 and are constrained with Modern-Era Retrospective Analysis for Research and Applications, Version 2 (MERRA-2).

In CTM-Fix, the emissions are based on the EDGAR 2000 inventory using the temporal scaling factors from Levin et al. (2010) (assuming a constant scaling after 2008) (Fig. 1a). In CTM the emissions are from EDGAR v4.2 (2011) and thus capture a substantial shift in SF<sub>6</sub> emissions from northern midlatitudes, over Europe and the United States, into the subtropics over Asia during 1997-2007 (Fig. 1b). In both simulations we integrate both SF<sub>6</sub> as well as an idealized NH "age-of-air" clock tracer, which is defined relative to a uniform source over 30°N-50°N.

## Results

### (1) Observed SF<sub>6</sub> Age: Mean and Variability

The meridional profile of  $\Gamma_{SF_6}$  at the surface features near-zero values over the NH midlatitude source region and increase sharply in the northern subtropics and tropics, increasing to ~1.5 yrs over southern middle and high latitudes (Waugh et al. (2013)).

Vertical profiles from ATom agree well with the NOAA/CCGG-based ages and reveal weak zonal variations between the Pacific and Atlantic oceans and weak vertical gradients (Fig. 2).

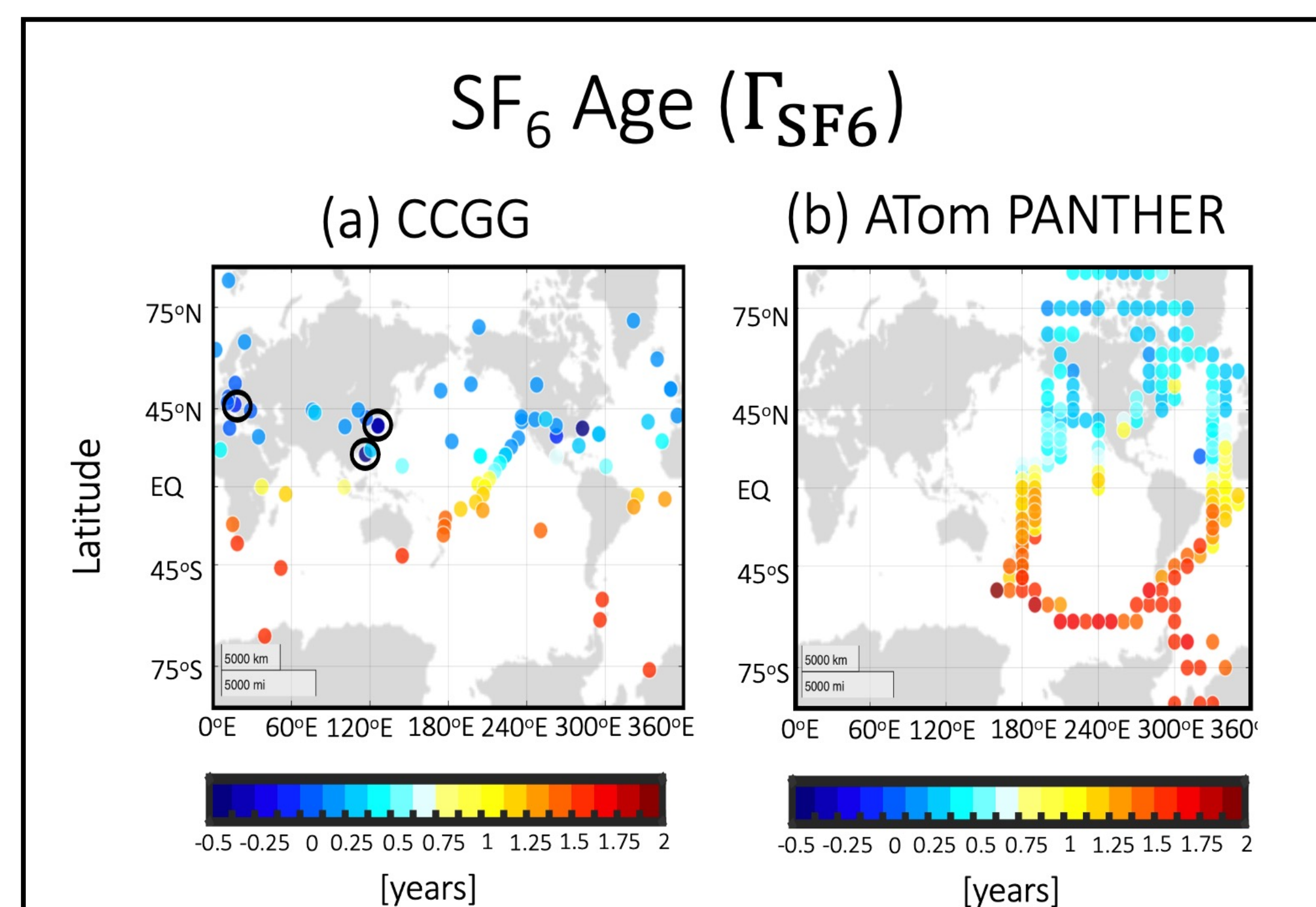


Figure 2: Climatological mean observed SF<sub>6</sub> age ( $\Gamma_{SF_6}$ ) derived from the NOAA/CCGG surface flask-air measurements (2008-2018) (a) and during ATom 1-4 for the PANTHER instrument (b). ATom-based ages have been averaged over pressures greater than 400 hPa. Black circles in (a) highlight sites over Europe (HUN) and Asia (DSI, TAP, AMY) where values of  $\Gamma_{SF_6}$  are most negative and where changes in SF<sub>6</sub> emissions are important for interpreting age trends over the 2000s.

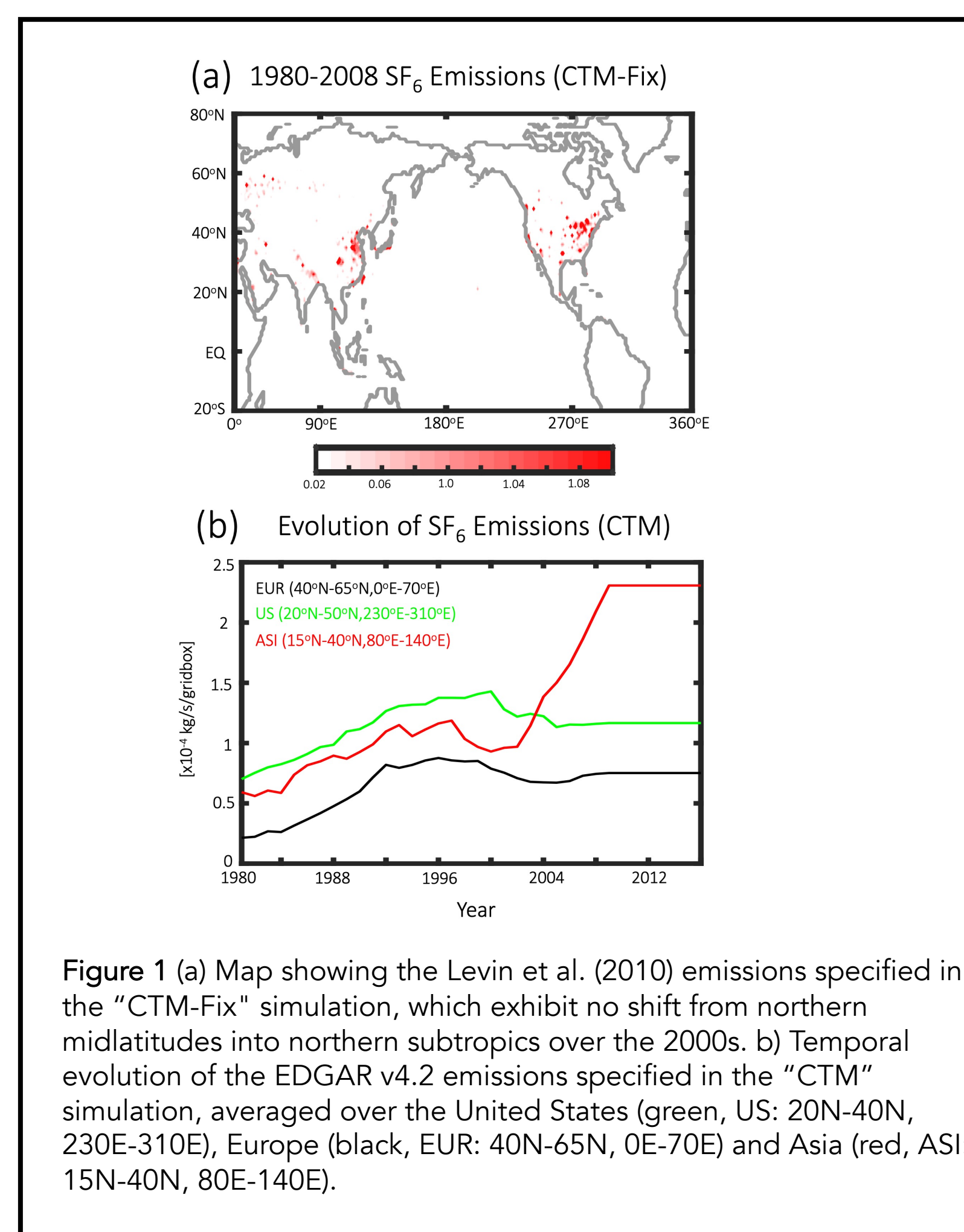


Figure 1 (a) Map showing the Levin et al. (2010) emissions specified in the "CTM-Fix" simulation, which exhibit no shift from northern midlatitudes into northern subtropics over the 2000s. (b) Temporal evolution of the EDGAR v4.2 emissions specified in the "CTM" simulation, averaged over the United States (green, US: 20N-40N, 230E-310E), Europe (black, EUR: 40N-65N, 0E-70E) and Asia (red, ASI: 15N-40N, 80E-140E).

By contrast, there are considerable zonal variations in the amplitude of the seasonal cycle of  $\Gamma_{SF_6}$  (Fig. 3a) associated with seasonal changes in the Intertropical Convergence Zone (ITCZ), with peak-to-peak amplitudes over the Indian Ocean ranging between 0.7-1.4 yr, compared to 0.3 yr over the Atlantic.

### (2) Observed SF<sub>6</sub> Age: Trends

Over the period 2000-2018 the SF<sub>6</sub> ages decrease south of the northern midlatitude source region (Fig. 3b). Over southern extratropical latitudes the trends in  $\Gamma_{SF_6}$  are -45(-0.12) days(yrs)/dec and are overall zonally uniform. These age trends are consistent with the interhemispheric exchange trends from Patra et al. (2011), but apply more generally to all surface latitudes south of 30°N and over a longer time period extending through 2018. We use the model simulations to understand the drivers of these observed age trends.

### (3) Modeled SF<sub>6</sub> Age: Driver of Biases

The model simulates much larger spatial variance in SF<sub>6</sub> over northern midlatitudes, compared to the observations (Fig. 4). Both simulations produce higher values of SF<sub>6</sub> over several sites spanning Europe, the United States and Southeast Asia, all of which are located near/downwind of emissions regions.

Better accounting for the bias in SF<sub>6</sub> (spatial) variance over northern midlatitudes substantially reduces the age bias in the model by ~50% from 0.3 yrs to 0.15 yrs. This is seen by comparing the age calculated with respect to the mean ( $[\chi]_{0,30N-60N}$ ) (Fig. 5a) versus the median ( $< \chi >_{0,30N-60N}$ ) (Fig. 5b) reference series. This suggests that age bias documented in previous studies is driven largely by biases in transport out of the northern midlatitude surface layer, although inaccurate emissions distributions may also be an important contributing factor.

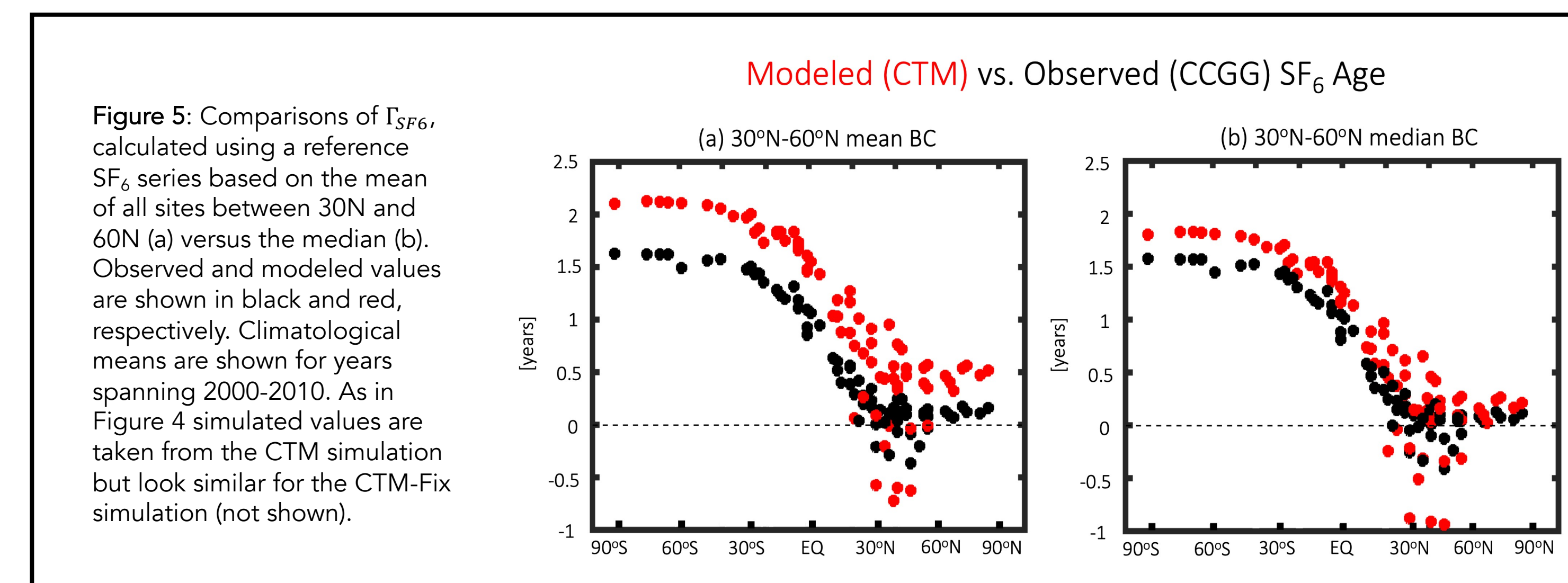


Figure 5: Comparisons of  $\Gamma_{SF_6}$ , calculated using a reference SF<sub>6</sub> series based on the mean of all sites between 30N and 60N (a) versus the median (b). Observed and modeled values are shown in black and red, respectively. Climatological means are shown for years spanning 2000-2010. As in Figure 4 simulated values are taken from the CTM simulation but look similar for the CTM-Fix simulation (not shown).

### (4) Modeled SF<sub>6</sub> Age: Driver of Observed Age Trends

Comparisons of CTM with CTM-Fix (Fig. 6) show that the observed  $\Gamma_{SF_6}$  trends are only captured in the simulation constrained with emissions that shift in time, suggesting that the age trends are primarily reflections of changes in emissions, not transport. This is supported further by the lack of any trends in the age-of-air tracer (green line).

## Conclusions

We have used new surface and aircraft measurements of SF<sub>6</sub> to present a more global picture of the climatological distribution, recent trends, and variability in the tropospheric SF<sub>6</sub> age. We have shown that:

#1.  $\Gamma_{SF_6}$  has decreased nearly uniformly south of northern midlatitudes by ~0.12 yr/dec over 2000-2018. These trends are primarily associated with a shift in emissions from northern midlatitudes into northern subtropics, and are not related to fundamental changes in transport.

#2. Models simulate larger spatial variance in SF<sub>6</sub> over northern midlatitudes, compared to observations. After accounting for this bias in simulated variance, the age bias reported in previous studies is substantially (50%) reduced.

Future work will focus on understanding the drivers of larger SF<sub>6</sub> variance in the models and on putting our results in the broader context of the models participating in the Chemistry Climate Modeling Initiative (CCMI).

C. Orbe, D. W. Waugh, S. Montzka, E. J. Dlugokencky, S. E. Strahan, S. D. Steenrod, S. Strode, J. W. Elkins, B. Hall, C. Sweeney, E. J. Hinsta, F. L. Moore, E. Penafiel, "Tropospheric Age-of-Air: Influence of SF<sub>6</sub> Emissions on Recent Surface Trends and Model Biases", In Press in *Journal of Geophysical Research: Atmospheres*.

D. W. Waugh, A. M. Crowell, E. J. Dlugokencky, G. S. Dutton, J. W. Elkins, B. D. Hall, E. J. Hinsta et al. "Tropospheric SF<sub>6</sub>: Age of air from the Northern Hemisphere midlatitude surface." *Journal of Geophysical Research: Atmospheres* 118, no. 19 (2013): 11-429.

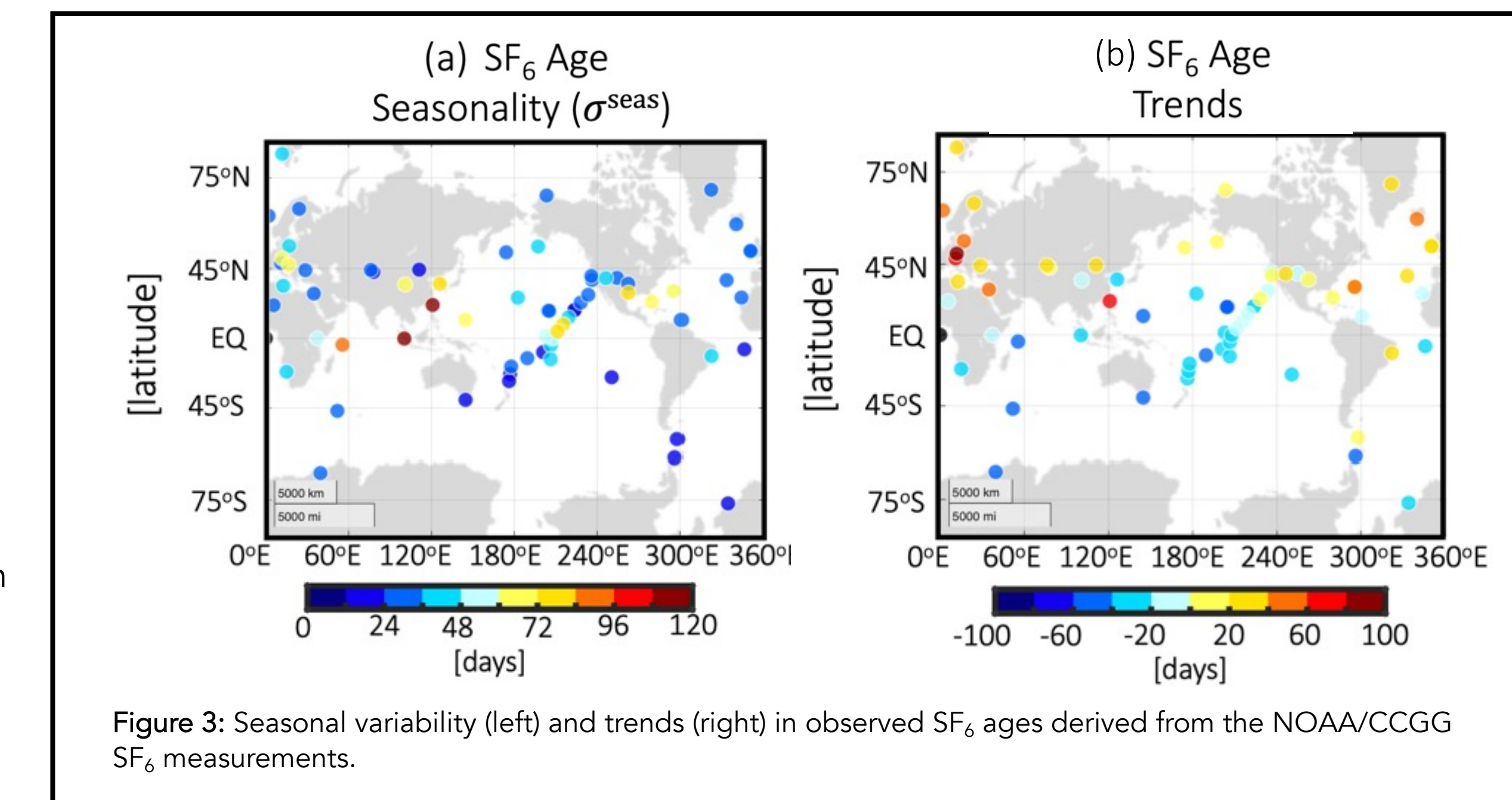


Figure 3: Seasonal variability (left) and trends (right) in observed SF<sub>6</sub> ages derived from the NOAA/CCGG SF<sub>6</sub> measurements.

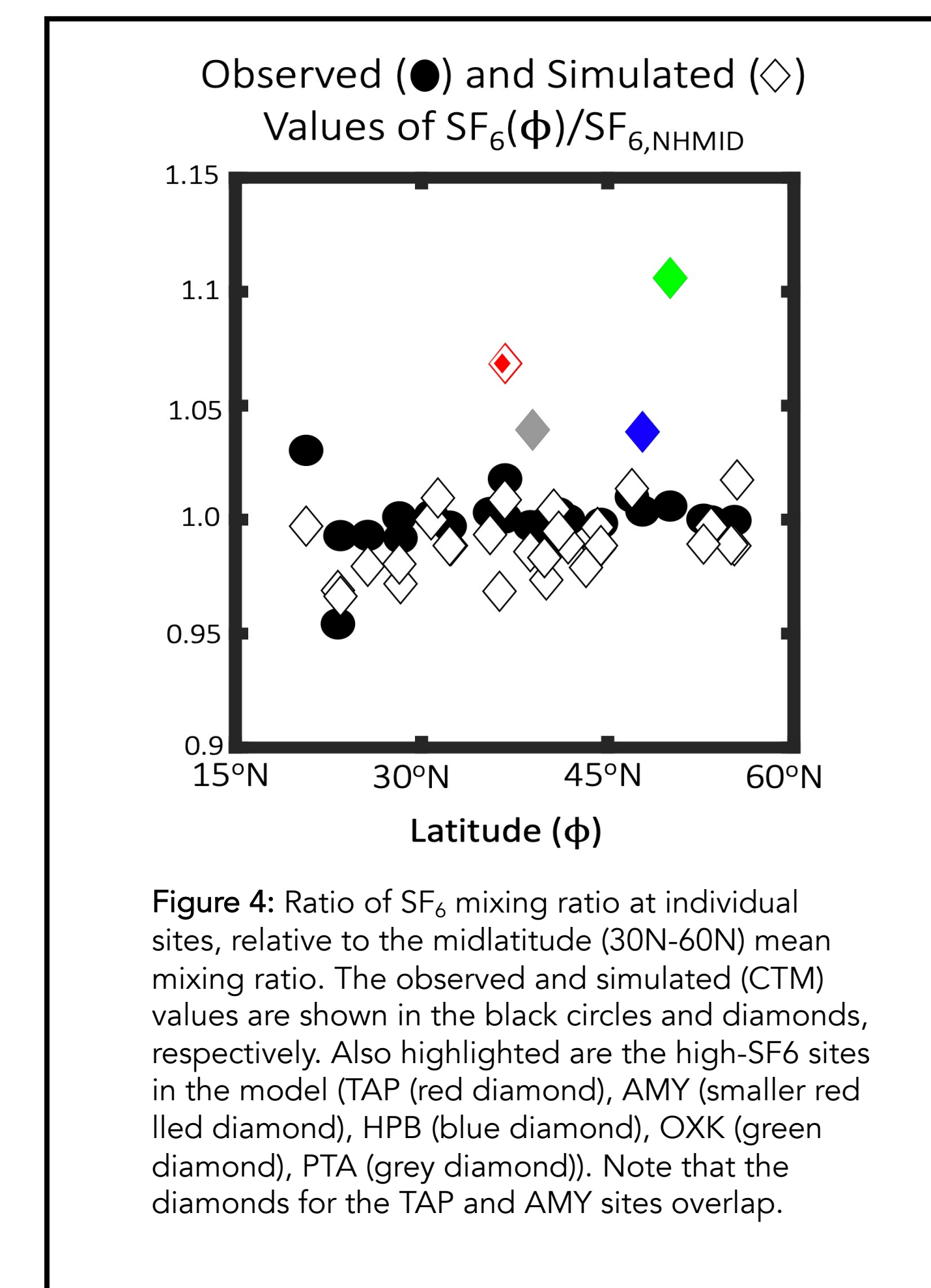


Figure 4: Ratio of SF<sub>6</sub> mixing ratio at individual sites, relative to the midlatitude (30N-60N) mean mixing ratio. The observed and simulated (CTM) values are shown in the black circles and diamonds, respectively. Also highlighted are the high-SF<sub>6</sub> sites in the model (TAP (red diamond), AMY (smaller red diamond), HPB (blue diamond), OXX (green diamond), PTA (grey diamond)). Note that the diamonds for the TAP and AMY sites overlap.

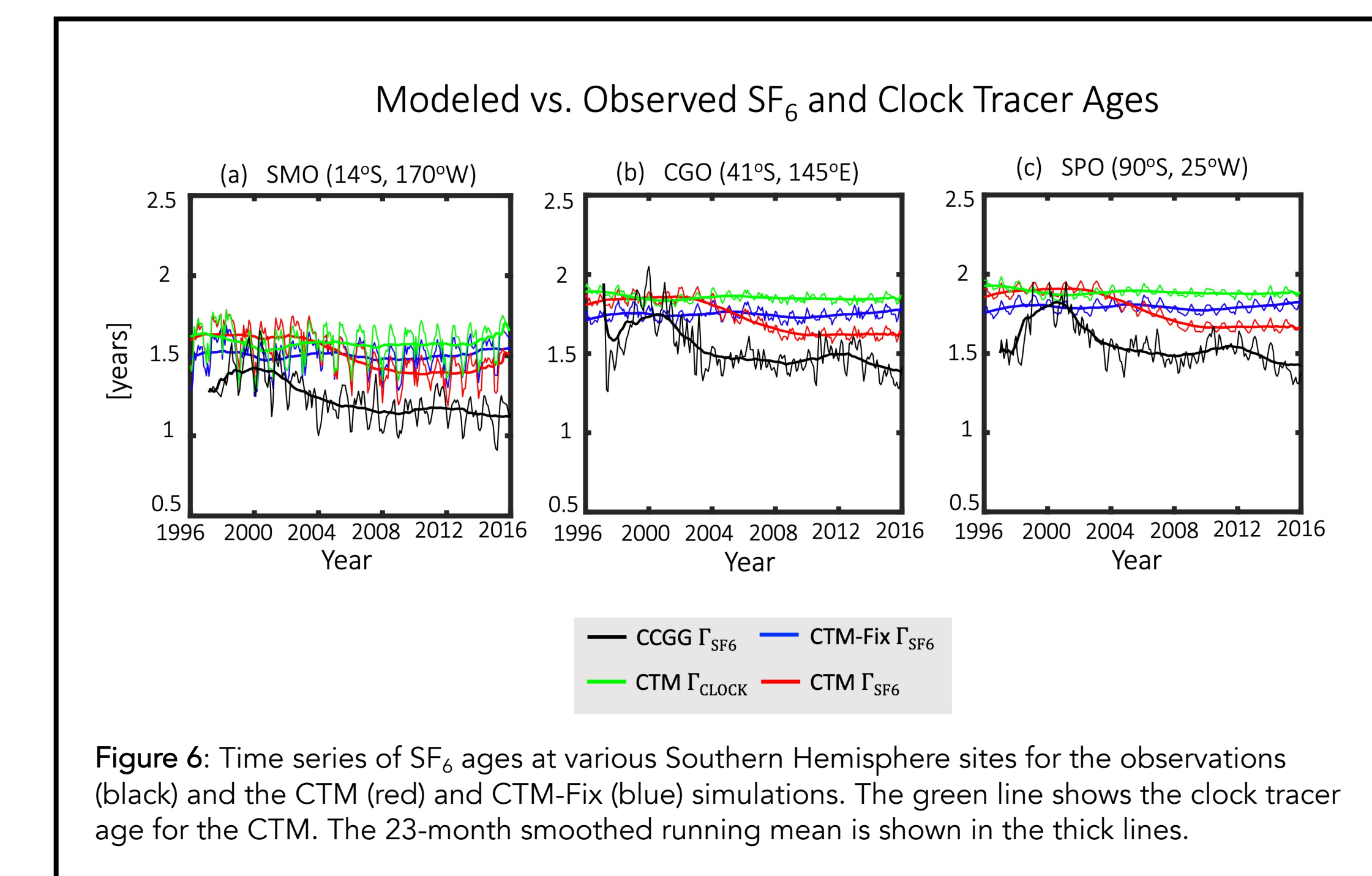


Figure 6: Time series of SF<sub>6</sub> ages at various Southern Hemisphere sites for the observations (black) and the CTM (red) and CTM-Fix (blue) simulations. The green line shows the clock tracer age for the CTM. The 23-month smoothed running mean is shown in the thick lines.